Nesprin-3 connects plectin and vimentin to the nuclear envelope of Sertoli cells but is not required for Sertoli cell function in spermatogenesis

Mirjam Ketema*, Maaike Kreft*, Pablo Secades, Hans Janssen, and Arnoud Sonnenberg
Division of Cell Biology, Netherlands Cancer Institute, 1066 CX Amsterdam, Netherlands

ABSTRACT **Nesprin-3 is a nuclear envelope protein that connects the nucleus to intermediate filaments by interacting with plectin. To investigate the role of nesprin-3 in the perinuclear localization of plectin, we generated nesprin-3–knockout mice and examined the effects of nesprin-3 deficiency in different cell types and tissues. Nesprin-3 and plectin are coexpressed in a variety of tissues, including peripheral nerve and muscle. The expression level of nesprin-3 in skeletal muscle is very low and decreases during myoblast differentiation in vitro. Of interest, plectin was concentrated at the nuclear envelope in only a few cell types. This was most prominent in Sertoli cells of the testis, in which nesprin-3 is required for the localization of both plectin and vimentin at the nuclear perimeter. Testicular morphology and the position of the nucleus in Sertoli cells were normal, however, in the nesprin-3–knockout mice and the mice were fertile. Furthermore, nesprin-3 was not required for the polarization and migration of mouse embryonic fibroblasts. Thus, although nesprin-3 is critical for the localization of plectin to the nuclear perimeter of Sertoli cells, the resulting link between the nuclear envelope and the intermediate filament system seems to be dispensable for normal testicular morphology and spermatogenesis.**

Monitoring Editor
Thomas M. Magin
University of Leipzig

Received: Feb 20, 2013
Revised: May 30, 2013
Accepted: May 31, 2013

INTRODUCTION

The nuclear interior is physically connected to the cytoskeleton by linker of nucleoskeleton and cytoskeleton (LINC) complexes situated in the nuclear envelope (NE; Crisp *et al.*, 2006; Razafsky and Hodzic, 2009). The main components of these complexes are SUN proteins present in the inner nuclear membrane and Klarsicht/ANC-1/Syne homology (KASH) domain–containing proteins located in the outer nuclear membrane. KASH proteins bind to the cytoskeleton and are localized at the NE by virtue of their conserved KASH domain. This C-terminal domain protrudes into the perinuclear space, the lumen between the two nuclear membranes, where it interacts with SUN proteins (Padmakumar *et al.*, 2005; Crisp *et al.*, 2006). SUN proteins, in turn, extend their N-termini in the nucleoplasm and can bind to nuclear lamins and chromosomes (Crisp *et al.*, 2006; Haque *et al.*, 2006; Ding *et al.*, 2007; Schmitt *et al.*, 2007).

Five KASH domain–containing proteins have been identified in vertebrates. The first proteins described were nesprin-1 and nesprin-2. The giant isoforms of these proteins are highly homologous to one another and share an N-terminal actin-binding domain (ABD) that allows them to establish a link between the NE and the actin cytoskeleton (Zhang *et al.*, 2001; Zhen *et al.*, 2002; Padmakumar *et al.*, 2004). In addition, nesprin-1 and nesprin-2 can interact with the plus and minus end–directed microtubule motor proteins kinesin and dynein (Fan and Beck, 2004; Zhang *et al.*, 2009; Schneider *et al.*, 2011; Yu *et al.*, 2011). Nesprin-3, nesprin-4, and KASH5 are much smaller and lack an ABD. Nesprin-3 interacts via its N-terminus with plectin, which in turn can bind to intermediate filaments (IFs; Wilhelmsen *et al.*, 2005). Nesprin-4 and KASH5 can associate with kinesin-1 and the dynein–dynactin complex, respectively, thereby linking the NE to

This article was published online ahead of print in MBoC in Press (http://www.molbiolcell.org/cgi/doi/10.1091/mbc.E13-02-0100) on June 12, 2013.

*These authors contributed equally to this work.

Address correspondence to: Arnoud Sonnenberg (a.sonnenberg@nki.nl).

Abbreviations used: ABD, actin-binding domain; IF, intermediate filament; KASH, Klarsicht/ANC-1/Syne homology; LINC, linker of nucleoskeleton and cytoskeleton; MEF, mouse embryonic fibroblast; MHC, myosin heavy chain; MTOC, microtubule-organizing center; NE, nuclear envelope; WT1, Wilms' tumor suppressor 1.

Supplemental Material can be found at:
http://www.molbiolcell.org/content/suppl/2013/06/10/mbc.E13-02-0100v1.DC1.html

microtubules (Roux *et al.*, 2009; Morimoto *et al.*, 2012). Hence their binding abilities enable KASH domain-containing proteins to connect the NE to all components of the cytoskeleton.

The presence of a nuclear–cytoskeletal connection suggests a role for KASH domain–containing proteins in maintaining shape and position of the nucleus. This is supported by studies in nesprin-1–mutant and nesprin-4–knockout mice, in which nuclear positioning was altered in skeletal muscle and outer hair cells, respectively (Grady *et al.*, 2005; Zhang *et al.*, 2007, 2010; Puckelwartz *et al.*, 2009; Horn *et al.*, 2013). Furthermore, nesprin-2 contributes to nuclear morphology (Kandert *et al.*, 2007; Lüke *et al.*, 2008) and is required for nuclear migration during the development of brain and retina (Zhang *et al.*, 2009; Yu *et al.*, 2011). More recently, KASH domain–containing proteins have also been implicated in mechanotransduction. A general disruption of the LINC complexes led to a reduction in intracellular force transmission and a concomitant decrease in cellular stiffness (Stewart-Hutchinson *et al.*, 2008; Wang *et al.*, 2009; Brosig *et al.*, 2010; Lombardi *et al.*, 2011). Nevertheless, despite our current knowledge of the role of KASH domain–containing proteins, little is known about the function of nesprin-3 (Ketema and Sonnenberg, 2011; Morgan *et al.*, 2011).

Nesprin-3 was initially identified in a yeast two-hybrid screen for binding partners of the cytoskeletal cross-linker protein plectin (Wilhelmsen *et al.*, 2005). Two isoforms have been described, nesprin-3α and nesprin-3β. Nesprin-3α can bind the ABD of plectin via a motif in its N-terminal spectrin repeat. Because nesprin-3β lacks such a motif, this isoform is unable to bind plectin (Wilhelmsen *et al.*, 2005; Postel *et al.*, 2011).

Plectin is a member of the plakin family and is characterized by the presence of several domains, such as an ABD, plakin domain, coiled-coil rod domain, and plakin repeats, which together provide plectin with highly versatile binding properties (McLean *et al.*, 1996; Wiche, 1998; Sonnenberg and Liem, 2007). The plakin repeats bind IFs, whereas the ABD can interact with F-actin, nesprin-3α, or the integrin β4 subunit in a mutually exclusive manner (Geerts *et al.*, 1999; Ketema *et al.*, 2007; Postel *et al.*, 2011). As such, plectin can establish connections between IFs and F-actin, the NE (via nesprin-3), or the plasma membrane (via β4). Overexpression and knockdown studies indicate that nesprin-3α recruits plectin to the NE and this recruitment is required for anchoring IFs at the NE (Wilhelmsen *et al.*, 2005; Morgan *et al.*, 2011; Postel *et al.*, 2011).

Because nesprin-3 is the only family member known to interact with IFs, complete redundancy in function with the other KASH domain–containing proteins is not expected. To investigate the function of nesprin-3, we previously generated nesprin-3–mutant zebrafish (Postel *et al.*, 2011). Despite reduced association of keratin filaments with the nucleus in epidermal cells of these zebrafish, no apparent gross abnormalities were observed. Yet, two recent reports showed that nesprin-3 is a determinant in both cell morphology and cell migration (Morgan *et al.*, 2011; Khatau *et al.*, 2012). Silencing of nesprin-3 led to a loss in coupling of the microtubule-organizing center (MTOC) to the nucleus. As a consequence, flow-induced MTOC polarization and migration were affected in human aortic endothelial cells (Morgan *et al.*, 2011). Furthermore, Khatau *et al.* (2012) showed that loss of nesprin-3 affected protrusion formation and migration in a three-dimensional (3D) collagen matrix.

To further explore the role of nesprin-3, we generated nesprin-3–knockout mice and analyzed the effect of nesprin-3 deficiency on the subcellular localization of plectin in different tissues and cell types. In addition, we investigated the role of nesprin-3 in in vitro cell migration.

RESULTS

Generation of nesprin-3–knockout mice

To generate nesprin-3–knockout mice, we used homologous recombination in embryonic stem cells to introduce loxP sites on either side of exon 2 in the nesprin-3 gene (*Syne3*; Figure 1A). Recombination in the embryonic stem cell clones was confirmed by Southern blotting (Figure 1B). One of the clones gave rise to chimeric offspring, which were crossed with FVB/N mice to generate *Syne3*$^{flox/flox}$ mice. Subsequent breeding with actin-Cre mice led to the generation of the *Syne3*$^{-/-}$ mouse strain. Deletion of exon 2 by Cre-mediated recombination between the loxP sites was confirmed by PCR on genomic DNA (Figure 1C). Because exon 2 contains the translation start sites for both nesprin-3α and the nesprin-3β isoform, the generated mice should be null mutants. This was verified by Western blot analysis on tissue lysates from *Syne3*$^{-/-}$ and wild-type littermates (Figure 1D). The *Syne3*$^{-/-}$ mice were born at Mendelian ratios and were indistinguishable from their wild-type littermates. Taken together, our data show that we successfully generated nesprin-3–knockout mice and that the mice were viable and fertile without any discernible abnormalities.

Loss of nesprin-3 has no or only minimal effect on the subcellular localization of plectin in most cell types

We previously demonstrated a role for nesprin-3 in the perinuclear localization of IFs in the zebrafish epidermis (Postel *et al.*, 2011). Although similar observations have been made in cell culture (Wilhelmsen *et al.*, 2005; Morgan *et al.*, 2011), it is largely undetermined to what extent nesprin-3 influences the subcellular localization of plectin and IFs in vivo.

To investigate the effect of nesprin-3 deficiency on the subcellular localization of plectin, we stained tissue sections of wild-type and nesprin-3–knockout littermates for nesprin-3 and plectin. Nesprin-3 and plectin are coexpressed in a large variety of cell types, but there are some notable exceptions. Whereas plectin was clearly present in keratinocytes and hepatocytes, these cells seem to lack expression of nesprin-3 (Figure 2A). Expression of nesprin-3 and plectin did coincide in striated muscle and the intestine, but colocalization was not observed in these tissues (Figures 2B and 3A). In addition, NE staining for nesprin-3 was relatively weak in cardiac muscle and only occasionally observed in skeletal muscle (Figure 3A).

In contrast to what might be anticipated, plectin was infrequently localized at the nuclear perimeter of nesprin-3–expressing cells. Some colocalization of nesprin-3 and plectin was found in the kidney, as well as in peripheral nerves. In the latter, nesprin-3 and plectin were coexpressed in Schwann cells (Figure 2C and Supplemental Figure S1). Loss of nesprin-3, however, did not have an obvious effect on the perinuclear localization of plectin (Figure 2C). The only exception thus far observed was in the testis and will be discussed later.

Taken together, the data indicate that although nesprin-3 and plectin are often coexpressed in cells, loss of nesprin-3 has only minimal effects on the subcellular localization of plectin. Of note, we occasionally observed a weak signal for nesprin-3 at the nuclear perimeter in cells of the nesprin-3–knockout mice. Although this most likely represents background staining, we cannot exclude that an as-yet-unidentified smaller isoform of nesprin-3 is still expressed at the NE in our knockout mice.

Nesprin-3 expression levels decrease during in vitro myogenic differentiation

During differentiation of skeletal muscle, mononucleated myoblasts fuse to form multinucleated myotubes. This process consists of a

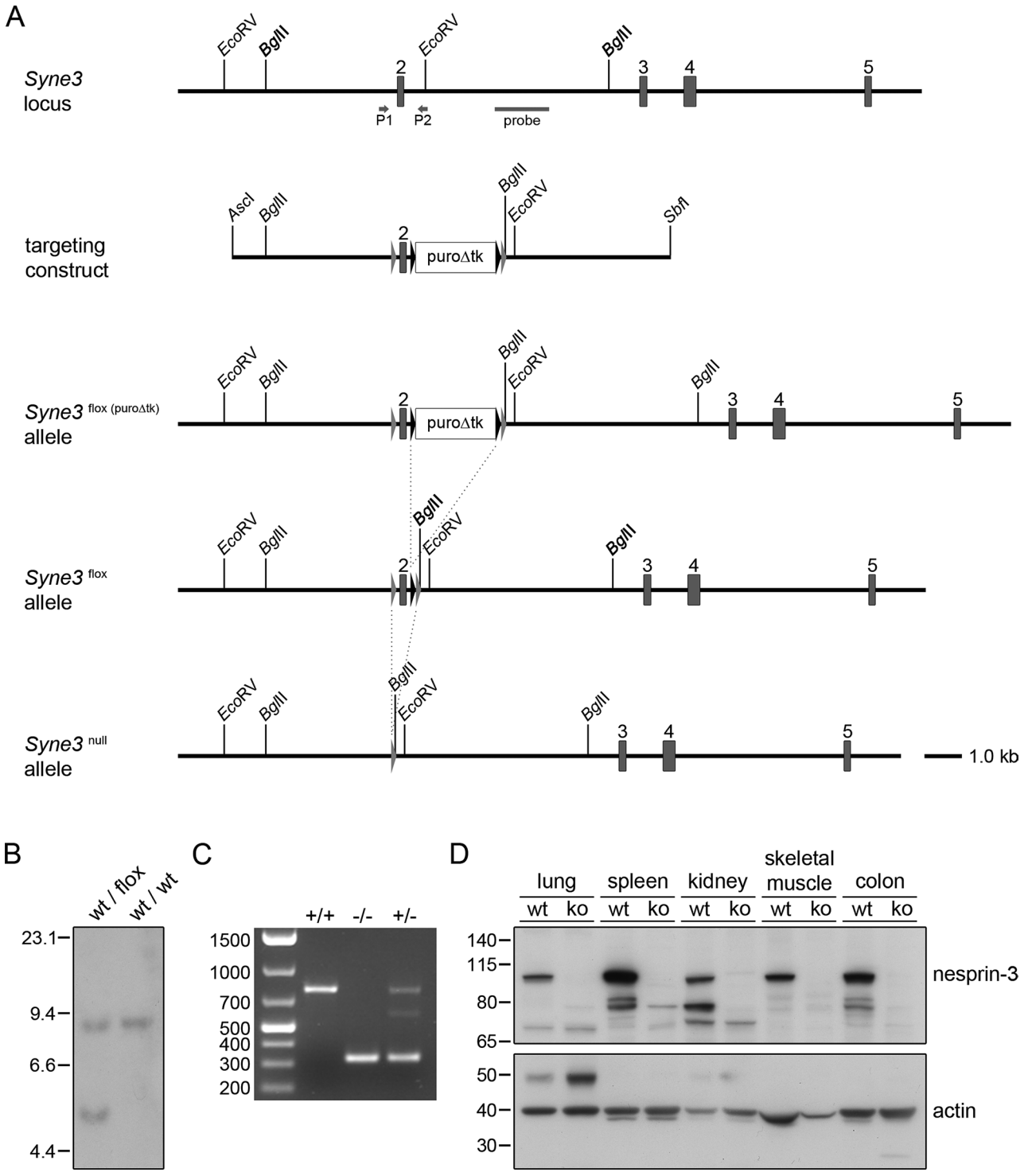

FIGURE 1: Targeting strategy and molecular analysis of recombinant embryonic stem cells and nesprin-3–knockout mice. (A) Partial *Syne3* gene structure, targeting construct, and different *Syne3* mutant alleles. Numbered gray boxes represent coding exons; gray and black triangles mark loxP and frt sites, respectively. Shown are the locations of the outermost 5′ and 3′ restriction sites used to generate the targeting construct and of *Eco*RV and *Bgl*II cleavage sites. The positions of the hybridization probe used for Southern blotting and the primers (arrows) used for the analysis of the different mutant alleles by PCR are indicated below the wild-type *Syne3* allele. Dotted lines indicate the FLPe- and Cre-specific recombination events. (B) Southern blot analysis of two independently targeted embryonic stem cell clones. Embryonic stem cell DNA was digested with *Bgl*II (bold), subjected to agarose gel electrophoresis, and transferred to nitrocellulose. We detected 9.2- and 5.3-kb fragments corresponding to wild-type and floxed alleles, respectively, by hybridization with a radiolabeled *Syne3* genomic probe. (C) PCR analysis of genomic DNA from wild-type (+/+), nesprin-3–knockout (–/–), and heterozygous (+/–) mice using primers P1 and P2. (D) Western blot analysis for the presence of nesprin-3 (top) in tissue lysates derived from wild-type (wt) and nesprin-3–knockout (ko) littermates. Actin levels (bottom) served as a loading control.

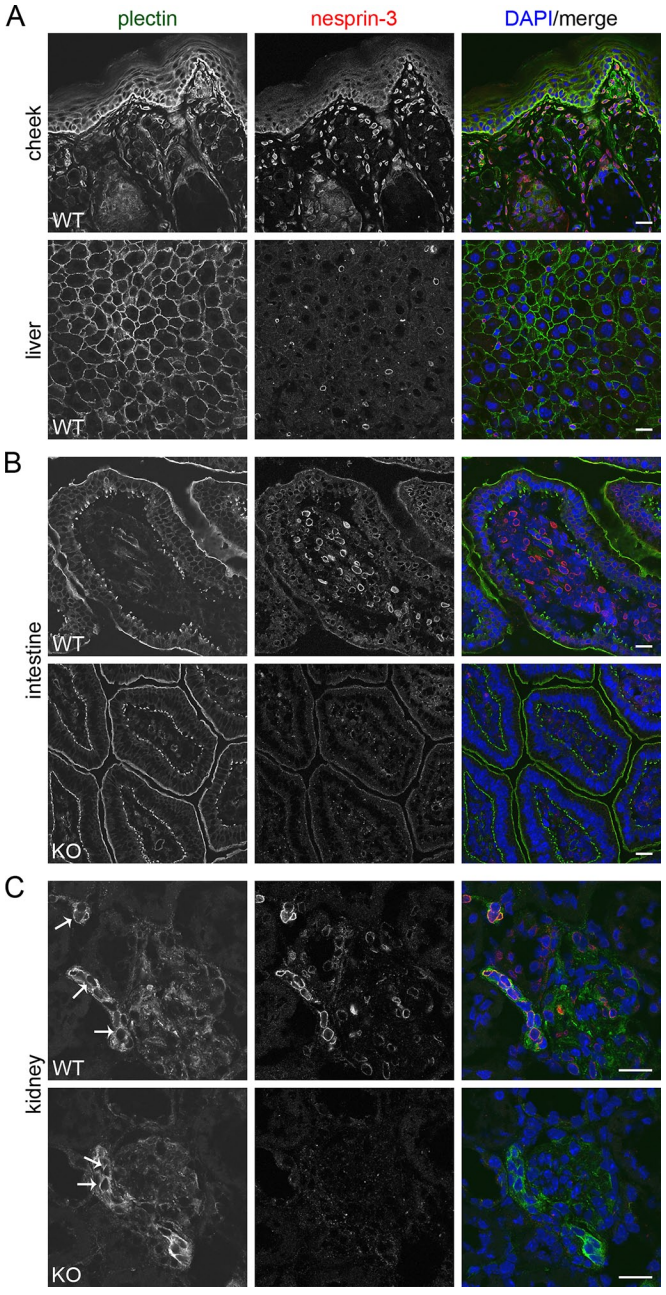

FIGURE 2: Distribution of nesprin-3 in mouse tissues. (A) Frozen sections of the liver and cheek of 5-wk-old wild-type mice were double labeled for plectin and nesprin-3. Nuclei were counterstained with DAPI. Scale bars, 20 µm. (B) Frozen sections of the intestines of 5-wk-old wild-type and nesprin-3–knockout littermates were stained for plectin and nesprin-3. Nuclei were counterstained with DAPI. Scale bars, 20 µm. (C) Frozen sections of the kidneys of 5-wk-old wild-type and nesprin-3–knockout littermates were double labeled for plectin and nesprin-3. Nuclei were counterstained with DAPI and perinuclear localization of plectin is indicated by arrows. Scale bars, 20 µm.

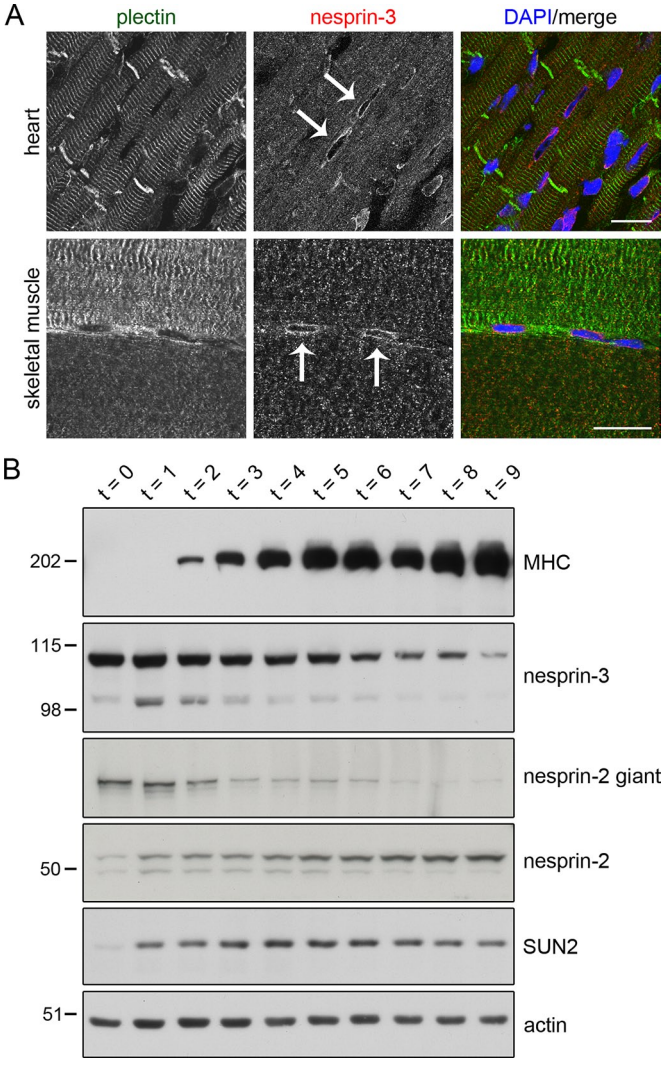

FIGURE 3: Expression of nesprin-3 decreases during myogenic differentiation. (A) Frozen sections of heart and skeletal muscle of 4-mo-old wild-type mice were stained for plectin and nesprin-3. Arrows indicate low expression of nesprin-3 at the NE. Scale bars, 20 µm. (B) C2C12 myoblasts were grown to confluence and differentiated into myotubes by a change in culture medium from 20% fetal calf serum to 2% horse serum. Cells were lysed at consecutive days after the induction of differentiation, and lysates were analyzed for expression of the indicated proteins. Actin levels served as a loading control. MHC, myosin heavy chain.

number of consecutive steps during which cells withdraw from the cell cycle and start to express muscle-specific genes, such as the one encoding myosin heavy chain (MHC; Rosenthal, 1989; Andrés and Walsh, 1996). The process ultimately results in the terminal differentiation of muscle cells and the formation of muscle fibers. To investigate the expression of nesprin-3 during myogenic differentiation, we used cells of the C2C12 myoblast cell line. When these cells reach confluence in culture, a change from growth medium to differentiation medium induces the formation of myotubes.

C2C12 cells were lysed at consecutive days after the induction of differentiation, and protein expression was analyzed by Western blot. As expected, the expression of MHC was induced during differentiation. It was first detectable after 2 d, and its level further increased in time (Figure 3B). In contrast, whereas nesprin-3 was strongly expressed in proliferating myoblasts, its expression level decreased during differentiation (Figure 3B). This is in line with our observation that nesprin-3 is virtually absent from skeletal muscle in mice.

We subsequently investigated the level at which some of the other LINC complex components are expressed. Similar to that of nesprin-3, the expression of nesprin-2 giant decreased upon differentiation (Figure 3B). This effect was not observed for all

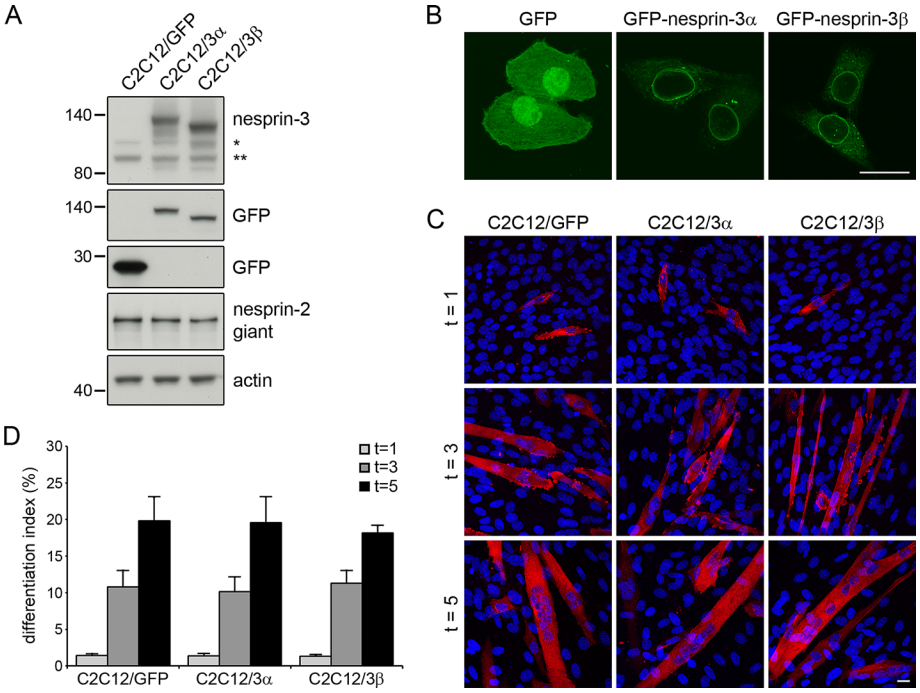

FIGURE 4: Myogenic differentiation is not affected by overexpression of nesprin-3. (A) Lysates of C2C12 myoblasts stably transfected with GFP (C2C12/GFP), GFP–nesprin-3α (C2C12/3α), and GFP–nesprin-3β (C2C12/3β) were analyzed by Western blot for expression of the indicated proteins. The GFP panels represent two parts of the same blot and therefore have an identical exposure time. Single and double asterisks indicate endogenous nesprin-3 and a nonspecific band, respectively. Actin levels served as a loading control. (B) C2C12/GFP, C2C12/3α, and C2C12/3β myoblasts were fixed in paraformaldehyde and analyzed by confocal microscopy to determine the localization of the GFP-tagged proteins. Scale bar, 20 μm. (C) C2C12/GFP, C2C12/3α, and C2C12/3β myoblasts were grown on gelatin-coated coverslips and differentiated for the indicated number of days. Cells were fixed in paraformaldehyde and stained for MHC (red) as a marker for differentiation. Nuclei were counterstained with DAPI (blue), and cells were analyzed by confocal microscopy. Scale bar, 20 μm. (D) Quantification of the results shown in C. The differentiation index is determined as the percentage of nuclei in MHC-positive cells over the total number of nuclei. Error bars represent the SD over three independent experiments.

nesprin-2 isoforms, as the expression of a ~50-kDa, smaller isoform, potentially corresponding to nesprin-2α_2 (Zhang *et al.*, 2005), increased in time (Figure 3B). Expression of SUN2 increased at day 1 and was maintained at the same level thereafter (Figure 3B).

To investigate whether down-regulation of nesprin-3 is an essential step during myogenic differentiation, we generated stable cell lines overexpressing green fluorescent protein (GFP; C2C12/GFP), GFP-nesprin-3α (C2C12/3α), or GFP-nesprin-3β (C2C12/3β). GFP-nesprin-3α and GFP-nesprin-3β were expressed to a similar extent, and both were localized at the NE of C2C12 myoblasts (Figure 4, A and B). Overexpression of nesprin-3 caused a displacement of endogenous nesprin-2 from the NE (data not shown) but did not alter the overall expression level of nesprin-2 giant (Figure 4A). The stable cell lines were stained for MHC after 1, 3, and 5 d of differentiation to determine their differentiation capacities (Figure 4C). Differentiation was quantified by determining the differentiation index, which is the percentage of nuclei in MHC-positive cells over the total number of nuclei. Surprisingly, the capacity of C2C12/3α and C2C12/3β to differentiate into myotubes was not affected (Figure 4, C and D). Hence myogenic differentiation does not require a reduction in the expression level of nesprin-3, nor does it require the localization of nesprin-2 at the NE in myoblasts.

Nesprin-3 and plectin are colocalized at the NE of Sertoli cells

Whereas nesprin-3 is virtually absent from skeletal muscle, it is strongly expressed at the NE of some basally located cells in the seminiferous epithelium of the testis, where it is colocalized with plectin (Figure 5A). A perinuclear localization pattern of plectin has been described in Sertoli cells of the rat testis (Guttman *et al.*, 1999). Sertoli cells are columnar-shaped epithelial cells that extend from the basement membrane to the lumen of the seminiferous tubules. These cells provide support and nutrition to the developing germ cells during all stages of spermatogenesis (Hess and Renato de Franca, 2008). Because Sertoli cell nuclei are localized at the basal side of the seminiferous epithelium, we sought to determine whether the nesprin-3–expressing cells in the testis are the Sertoli cells. Frozen sections of the testis of a wild-type mouse were stained for plectin and Wilms' tumor suppressor 1 (WT1), which can serve as a marker for Sertoli cells (Del Rio-Tsonis *et al.*, 1996; Myers *et al.*, 2005). Perinuclear localization of plectin was exclusively observed around WT1-positive nuclei (Figure 5B), indicating that the nesprin-3–expressing cells in the testis are indeed the Sertoli cells.

Localization of plectin and vimentin at the NE of Sertoli cells depends on nesprin-3

Because nesprin-3 and plectin are colocalized at the NE of Sertoli cells, we sought to determine whether the localization of plectin at this site depends on the presence of nesprin-3. We therefore analyzed frozen sections of the testes of wild-type and nesprin-3–knockout littermates. As expected, nesprin-3 was localized at the NE of Sertoli cells in wild-type mice, but no nesprin-3 could be detected in the nesprin-3–knockout testis (Figure 6A). To recognize the Sertoli cell nuclei in the absence of nesprin-3, we tested other LINC complex components for their presence at the NE. Like nesprin-3, nesprin-2 was expressed at the NE of Sertoli cells (Figure 6B). Moreover, because nesprin-2 was not detected at the NE of germ cells, it could function as a Sertoli cell marker in our further studies. We subsequently examined the localization of plectin in the testis of nesprin-3–knockout mice. In the absence of nesprin-3, plectin was no longer associated with the NE (Figure 6B), suggesting that plectin is indeed recruited to the nuclear perimeter by nesprin-3.

Nesprin-3 and plectin establish a link between the NE and the IF system. We therefore investigated the localization of IFs in the testis of nesprin-3–knockout mice. Because the main type of IF present in Sertoli cells is vimentin (Franke *et al.*, 1979), frozen sections of the testis were double labeled for vimentin and plectin. Furthermore, the sections were also stained for the laminin-α1 chain, which is one of the main basement membrane components in the seminiferous epithelium (Durbeej *et al.*, 1998; Häger *et al.*, 2005). Whereas vimentin is clearly present at the nuclear perimeter of wild-type Sertoli cells, it is not in Sertoli cells from nesprin-3–knockout mice

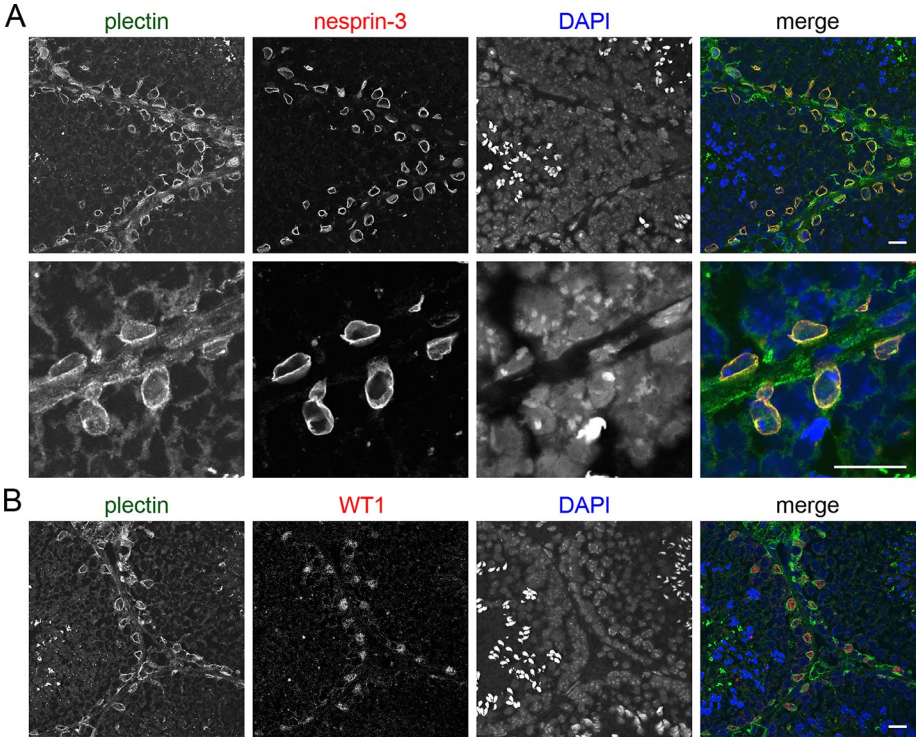

FIGURE 5: Nesprin-3 and plectin colocalize at the NE of Sertoli cells. (A) Frozen sections of the testis of a 2-mo-old wild-type mouse were stained for nesprin-3 and plectin. Nuclei were counterstained with DAPI. Scale bars, 20 μm. (B) Frozen section of the testis of a 2-mo-old wild-type mouse stained for plectin and WT1. Nuclei were counterstained with DAPI. Scale bar, 20 μm.

(Figure 6C). In contrast, the organization of microtubules and F-actin was not affected by the loss of nesprin-3 (data not shown). These results indicate that nesprin-3 and plectin are indeed responsible for the establishment of a link between the NE and the IF system in Sertoli cells.

Nuclear positioning in Sertoli cells is not affected by loss of nesprin-3

Nuclei of Sertoli cells are normally located close to the basement membrane. Because nesprin-3 and plectin establish a link between the NE and the IF cytoskeleton, loss of this link in nesprin-3–knockout mice might affect the localization of Sertoli cell nuclei. To investigate possible effects on nuclear positioning, we stained testis sections of wild-type and nesprin-3–knockout mice for WT1 as a marker for nuclei in Sertoli cells. In wild-type mice, the nuclei were mainly located along the basal side of the seminiferous epithelium, with the exception of a limited number of nuclei (15.6 ± 2.6%) in a more nonbasal position (Figure 7, A and B). Loss of nesprin-3 did not affect the position of nuclei in Sertoli cells, as the percentage of nuclei in a nonbasal position (18.0 ± 5.7%) was not significantly different from that in wild-type mice ($p = 0.48$; Figure 7B). Similar observations were made by electron microscopy, which revealed a close juxtaposition between Sertoli cell nuclei and the basement membrane in both wild-type and nesprin-3–knockout mice (Figure 7C). Hence nesprin-3 does not appear to be required for nuclear positioning in Sertoli cells.

It was suggested that nesprin-3–containing LINC complexes have a role in spermatogenesis by mediating elongation of the spermatid nucleus (Göb *et al.*, 2010). Immunofluorescence analysis of testis cryosections, however, did not reveal staining for nesprin-3 in germ cells. Furthermore, there were no gross defects in spermatid elongation in the nesprin-3–knockout mice (Figure 7D). Together with the observations that the knockout mice were fertile and that the structural organization of the testis was normal (Figure 7A), these results suggest that nesprin-3 does not play a role in spermatogenesis.

We previously proposed the existence of a continuous protein scaffold between the extracellular matrix and the nuclear interior in which IFs are attached to the nucleus via nesprin-3 and to hemidesmosomes through the action of integrin α6β4 (Wilhelmsen *et al.*, 2005). To investigate whether there is such a continuous link in Sertoli cells, we stained tissue sections of wild-type testes for multiple integrin subunits. Unexpectedly, we found no evidence for the expression of the integrin β4 subunit in the testis (data not shown). In contrast, α6 and β1 were expressed at the basal side of the seminiferous epithelium (Figure 6, D and E). Moreover, the distribution of the integrin α6 subunit was patchy along the basement membrane, with more intense staining in the presence of Sertoli cells (Figure 6E). These results suggest that the basal cell surface of Sertoli cells is not connected by α6β4 to the IF system but instead by α6β1 to the actin cytoskeleton.

Nesprin-3 is the main protein responsible for the association of vimentin with the NE

Association of plectin and vimentin with the NE of Sertoli cells is clearly dependent on nesprin-3. In contrast, loss of nesprin-3 had only minor effects on the localization of plectin and IFs in other tissues. To determine whether other KASH domain–containing proteins are involved in the attachment of IFs to the NE, we investigated the localization of vimentin in mouse embryonic fibroblasts (MEFs) derived from wild-type and nesprin-3–knockout littermates. Loss of nesprin-3 resulted in a clear but incomplete reduction in the percentage of cells with NE-associated vimentin (Figure 8, A and B). Moreover, the extent to which vimentin filaments align with the NE in individual nesprin-3–knockout cells was always less than that observed in wild-type cells (data not shown). Overexpression of GFP-tagged, dominant-negative nesprin-1 (KASH1), which is known to displace all endogenous KASH domain–containing proteins from the NE (Stewart-Hutchinson *et al.*, 2008; Lombardi *et al.*, 2011), did not significantly decrease the percentage of cells whose NE was associated with vimentin when compared with nesprin-3–deficient cells ($p = 0.55$; Figure 8, A and B). Thus nesprin-3 is the only KASH protein that mediates the linkage of IFs to the NE in MEFs.

Nesprin-3 is not required for migration and polarization of MEFs

LINC complexes were shown to be involved in cell migration and polarization (Lombardi *et al.*, 2011). These observations were made after transfection of cells with a dominant-negative KASH construct. Whereas several studies indicate that nesprin-1 and -2 are the primary KASH proteins involved in cell migration (Lüke *et al.*, 2008; Chancellor *et al.*, 2010; Luxton *et al.*, 2010; Rashmi *et al.*, 2012), two

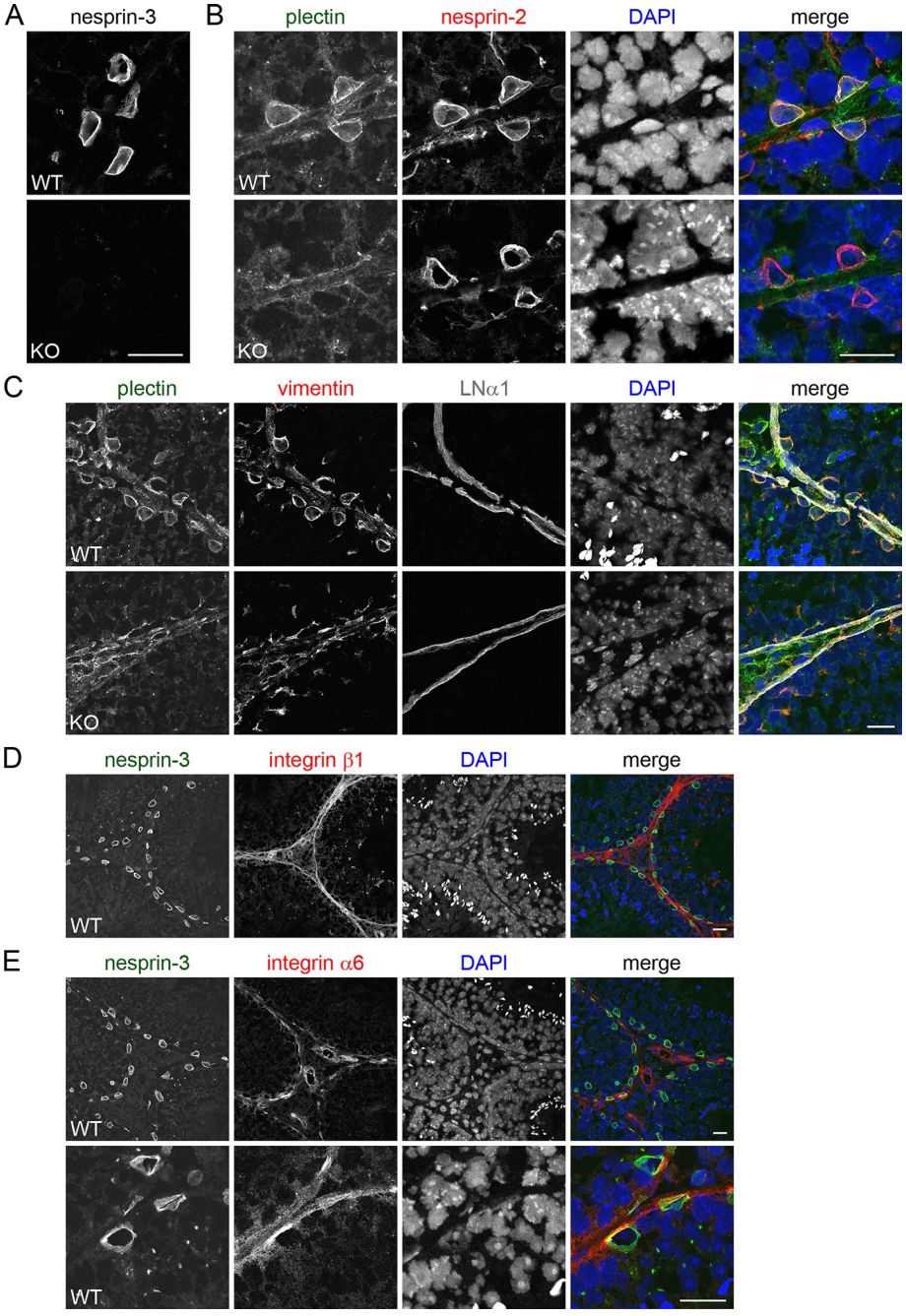

FIGURE 6: Loss of plectin and vimentin from the nuclear perimeter in Sertoli cells of nesprin-3–knockout mice. (A–C) Frozen sections of the testes of 2-mo-old wild-type (WT) and 2-mo-old nesprin-3–knockout (KO) mice were stained for nesprin-3 (A), double labeled for plectin and nesprin-2 (B), or stained for a combination of plectin, vimentin, and the laminin α1 chain (LNα1) (C). Nuclei were counterstained with DAPI. Scale bar, 20 μm. (D, E) Frozen sections of the testis of a 2-mo-old wild-type mouse were double-labeled for nesprin-3 and either the integrin β1 (D) or the integrin α6 (E) subunit. Nuclei were counterstained with DAPI. Scale bars, 20 μm.

recent studies demonstrated a similar role for nesprin-3 (Morgan *et al.*, 2011; Khatau *et al.*, 2012).

To investigate the role of nesprin-3 in cell migration, primary MEFs derived from two wild-type (MEF8, MEF10) and two nesprin-3–knockout (MEF3, MEF9) littermates were subjected to an in vitro scratch assay (Figure 9A). Time-lapse imaging of the wounded monolayers indicated that both wild-type and nesprin-3–knockout cells closed the wound after ~20 h (Figure 9B). Moreover, a determination of the speed at which the wound surface is covered revealed no significant differences between wild-type and nesprin-3–deficient MEFs (Figure 9C), indicating that nesprin-3 is not required for cell migration.

The reduction in flow-induced migration reported by Morgan *et al.* (2011) after down-regulation of nesprin-3 was associated with an increase in the distance between the MTOC and the NE and a defect in cell polarization. To investigate whether the distance between the MTOC and the nucleus was affected in our model system, we stained wild-type and nesprin-3–deficient MEFs for γ-tubulin and lamin B to identify the MTOC and NE, respectively (Supplemental Figure S2A). Of interest, the average distance between the MTOC and the nucleus observed in our primary nesprin-3–knockout MEFs was not significantly different from that seen in the wild-type MEFs ($p = 0.56$) (Supplemental Figure S2B). Furthermore, in line with our observation that cell migration was not affected in the nesprin-3–knockout MEFs, we observed normal induction of MTOC polarization upon scratch wounding (Figure 9D).

To demonstrate a possible involvement of other KASH domain–containing proteins in cell polarization, we used nesprin-3–deficient cells overexpressing either GFP–nesprin-3β (MEF3/3β) or GFP–dominant-negative nesprin-1 (MEF3/KASH1). Overexpression of GFPxnesprin-3β had a variable effect on cell polarization. Individually generated MEF3/3β cell lines showed a normal or a partially impeded reorientation of the MTOC after scratch wounding (Figure 9E). In contrast, MTOC polarization was completely lost in MEF3/KASH1 cells (Figure 9E). These results strongly correlate with the extent to which the GFP-tagged constructs displace other endogenous KASH domain–containing proteins from the NE (Supplemental Figure S3), suggesting that KASH proteins other than nesprin-3 are required for cell polarization in MEFs.

DISCUSSION

We generated nesprin-3–knockout mice to investigate the role of nesprin-3 in the perinuclear localization of plectin. Although nesprin-3 and plectin are often coexpressed in cells, colocalization of the two proteins was only occasionally observed and found to be most prominent in Sertoli cells of the testis. In fact, nesprin-3 was essential for the recruitment of both plectin and vimentin to the nuclear perimeter of Sertoli cells. Whereas our study provides the first in vivo proof of nuclear localization of plectin by nesprin-3, its loss in nesprin-3–knockout mice did not result in an abnormal phenotype. Furthermore, in vitro cell migration and polarization also were not

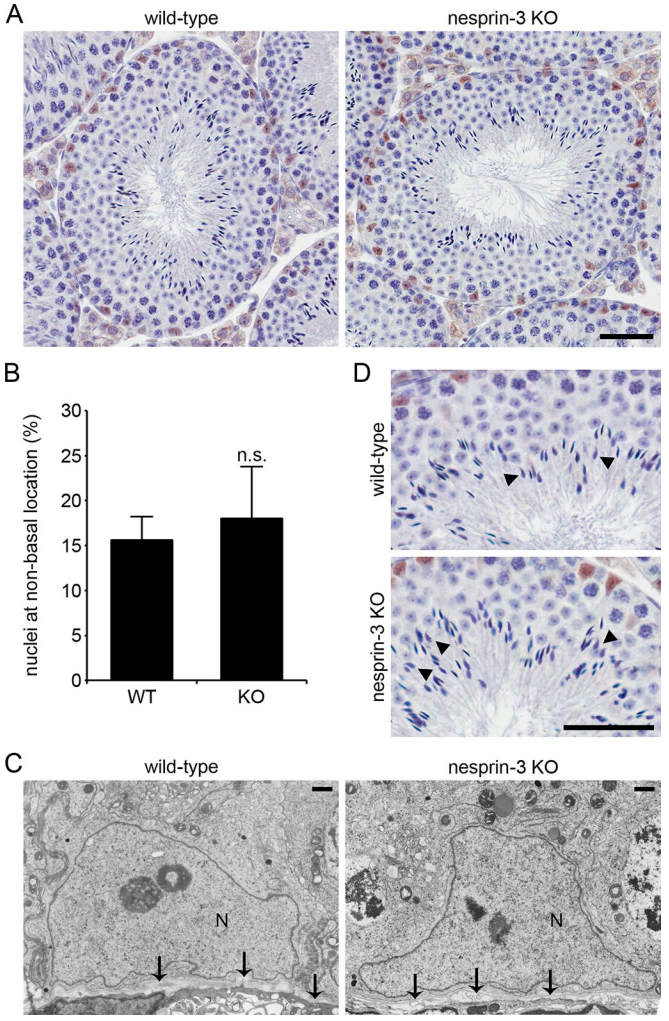

FIGURE 7: Nuclear positioning in Sertoli cells is not affected by loss of nesprin-3. (A) Testis sections of 2.5-mo-old wild-type and nesprin-3–knockout littermates were stained for WT1 (brown) and counterstained with hematoxylin. Scale bar, 50 μm. (B) Quantification of Sertoli cell nuclear positioning in cross sections of the testis. The localization of Sertoli cell nuclei was scored as either basal or nonbasal for four mice each group. More than 800 nuclei/mouse were analyzed. Error bars indicate the SD. (C) Representative electron microscopy images of Sertoli cell nuclei (N) from 2-mo-old wild-type and nesprin-3–knockout littermates. The basement membrane is indicated by arrows. Scale bars, 1 μm. (D) Testis sections of 2.5-mo-old wild-type and nesprin-3–knockout littermates were stained as described in A. Arrowheads indicate spermatids with an elongated and falciform shape of the nucleus. Scale bar, 50 μm.

affected by the loss of nesprin-3. Our data do indicate, however, the involvement of other KASH proteins in these last processes.

The lack of an abnormal phenotype in nesprin-3–knockout mice is not unexpected. We previously described the normal development of nesprin-3–mutant zebrafish (Postel *et al.*, 2011). Furthermore, in preliminary studies nesprin-3–knockout mice had no apparent abnormalities, and neuronal migration in the brain of these mice was normal (Zhang *et al.*, 2009; Starr and Fridolfsson, 2010). Despite the absence of gross abnormalities, the knockout mice allowed us to investigate the function of nesprin-3 in Sertoli cells.

As the only somatic cell type present in the testis, Sertoli cells give structure to the seminiferous epithelium and guide the

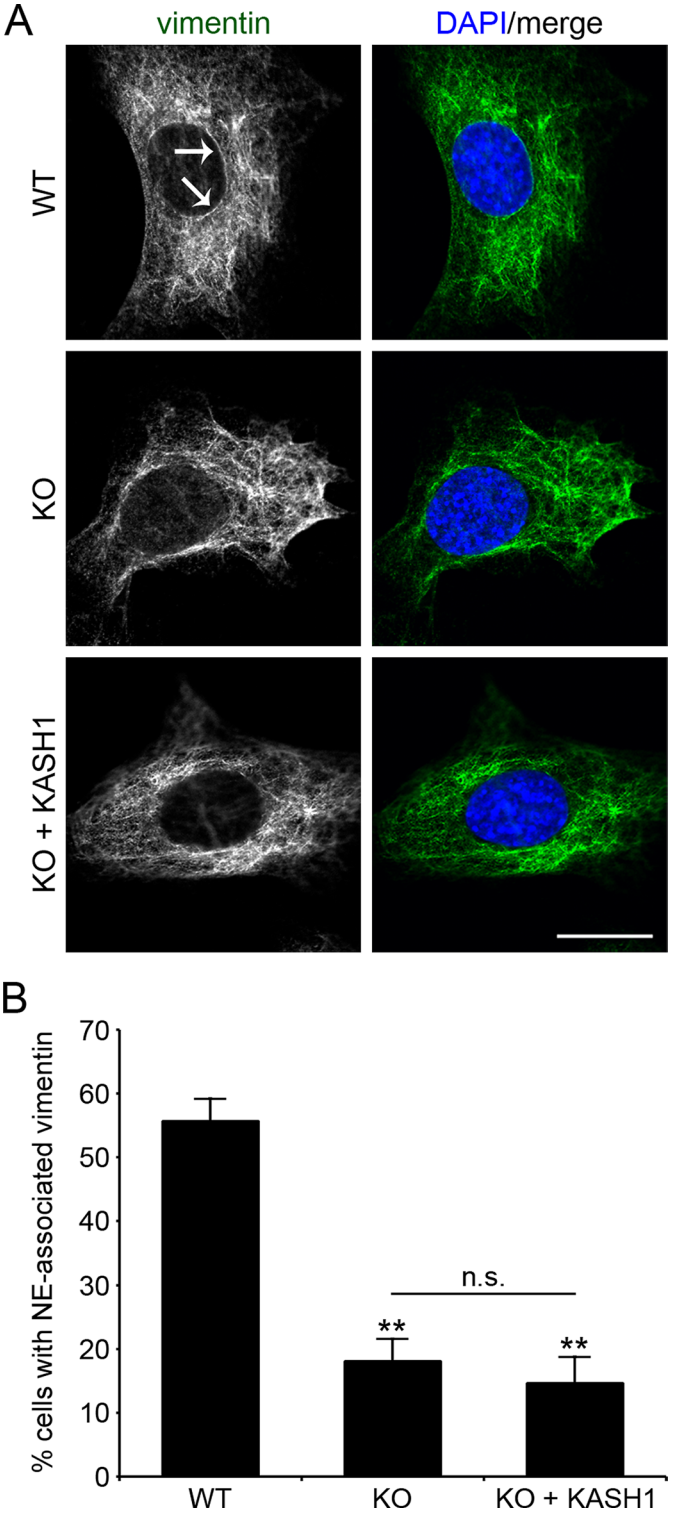

FIGURE 8: Association of vimentin with the NE is primarily mediated by nesprin-3. (A) Immortalized MEFs were fixed in paraformaldehyde and stained for vimentin. Nuclei were counterstained with DAPI, and cells were analyzed by confocal microscopy. NE-associated vimentin is indicated by arrows. WT, wild-type; KO, nesprin-3 knockout; KO + KASH1, nesprin-3 knockout stably expressing GFP–dominant-negative nesprin-1 (KASH1). Scale bar, 20 μm. (B) Percentage of cells with NE-associated vimentin. Error bars indicate the SD over three experiments. For each experiment 100 cells/sample were analyzed. $^{**}p < 0.001$.

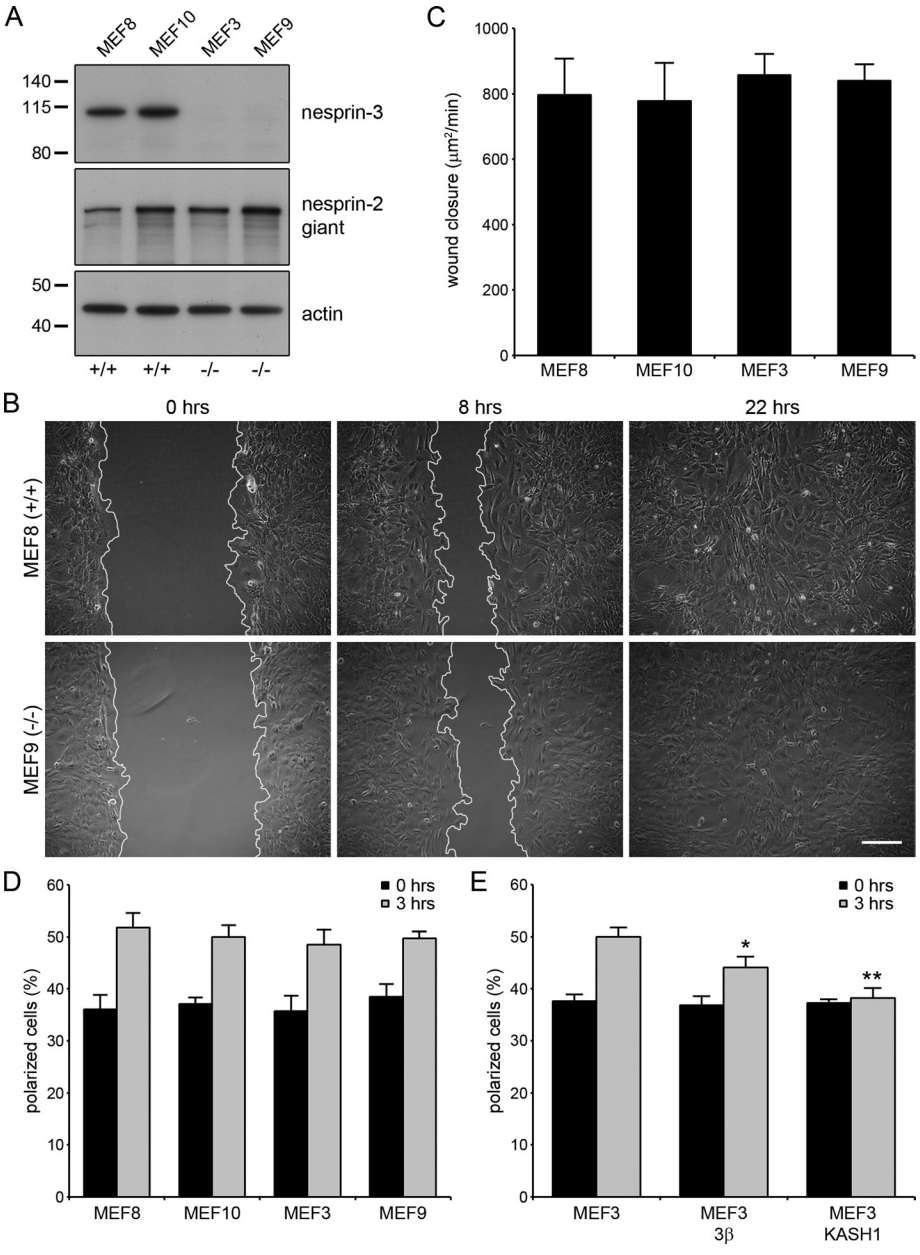

FIGURE 9: Nesprin-3 is not required for cell migration and polarization of MEFs. (A) Lysates of wild-type (MEF8, MEF10) and nesprin-3$^{-/-}$ (MEF3, MEF9) cells were analyzed by Western blot for expression of the indicated proteins. Actin levels served as a loading control. (B) Phase contrast images of wild-type (MEF8) and nesprin-3$^{-/-}$ (MEF9) cells at 0, 8, and 22 h postwounding. Wound edges are marked in white. Scale bar, 200 μm. (C) Rate of wound closure in wild-type (MEF8, MEF10) and nesprin-3$^{-/-}$ (MEF3, MEF9) cells. Error bars indicate the SD in one representative experiment. $n = 4$ for MEF10 and $n = 6$ for MEF3, MEF8, and MEF9. (D, E) Percentage of polarized cells at 0 and 3 h postwounding. Polarization was determined in primary (D) and immortalized cells (E) by determining the orientation of the MTOC with respect to the wound edge. Error bars indicate the SD. *$p < 0.05$; **$p < 0.001$.

developing germ cells through all stages of spermatogenesis. Plectin and vimentin are both concentrated at the nuclear perimeter of Sertoli cells (Amlani and Vogl, 1988; Aumüller *et al.*, 1988; Guttman *et al.*, 1999), and it was suggested that plectin participates in the linkage of vimentin to the NE (Guttman *et al.*, 1999). Our observation that the loss of nesprin-3 affects the distribution of plectin and vimentin in the nuclear vicinity supports this proposal.

Despite its dramatic effect on the localization of plectin and vimentin, nuclear positioning and testicular morphology were found to be normal in the nesprin-3–knockout mice. Hence the attachment of IFs to the nucleus did not appear to be required for normal function of Sertoli cells in spermatogenesis. Consistently, the morphology of the seminiferous epithelium was also unaffected in vimentin-knockout mice (Vogl *et al.*, 1996). Regardless of the complete absence of IFs, the Sertoli cells exhibited a normal differentiated phenotype with a basal localization of the nuclei, and the mice reproduced normally (Colucci-Guyon *et al.*, 1994; Vogl *et al.*, 1996).

IFs provide tensile strength to cells for resisting mechanical stress (Fuchs and Cleveland, 1998; Magin *et al.*, 2000). The work of Vogl *et al.* (1996) suggests that this is also true for the seminiferous epithelium; the mechanical damage observed in immersion-fixed material from vimentin-knockout mice was much higher than the fixation-induced damage observed in wild-type material. It is unclear, however, how mechanical trauma during fixation is related to physiological traumas experienced in vivo. Furthermore, it remains to be determined whether the mechanical damage is caused by the loss of vimentin from the nuclear vicinity or by its absence from cell junctions and a general decrease in the stability and elasticity of the cytoskeleton.

Our results demonstrate that nesprin-3 mediates a link between the NE and the IF system, but we were unable to show a continuation of this link to the extracellular matrix through hemidesmosomes, as we previously suggested in keratinocytes (Wilhelmsen *et al.*, 2005). Although small hemidesmosome-like junctions have been described in Sertoli cells (Wrobel *et al.*, 1979; Zhu *et al.*, 1997; Siu and Cheng, 2004), we could not detect the integrin β4 subunit in sections of the testis or in a Sertoli cell line in culture (data not shown). The attachment of Sertoli cells to the basement membrane could in part be mediated by α6β1. This integrin is expressed in the seminiferous epithelium and is known to anchor the actin cytoskeleton to the plasma membrane. Given that actin filaments can also be connected to the nucleus via nesprin-2 (Zhen *et al.*, 2002; Luxton *et al.*, 2010), this KASH domain–containing protein might play a role in the positioning of nuclei in Sertoli cells.

Whereas nesprin-3 is required for the localization of plectin and vimentin at the nuclear perimeter of Sertoli cells, loss of nesprin-3 did not appear to affect the localization of these proteins in other tissues. It is possible that in some of these tissues the loss of plectin association with the NE is obscured by a high level of plectin expression in the cytoplasm. Furthermore, plectin may be sequestered

away from the nucleus by binding to one or more high-affinity binding partners, for example, integrin β4 (Geerts *et al.*, 1999). The finding that the perinuclear localization of vimentin is altered in nesprin-3–deficient MEFs clearly demonstrates that the role of nesprin-3 in linking IFs to the nucleus is not restricted to Sertoli cells. We found no evidence for a role of other KASH proteins in the localization of plectin/IFs at the NE, although a minor contribution of other non-KASH proteins cannot be excluded.

In this study, we showed a decrease in the expression level of nesprin-3 during the differentiation of C2C12 myoblasts into myotubes. This decrease in protein level is most likely caused by a decrease of gene expression, as it was previously demonstrated that nesprin-3 (NET53) mRNA levels decrease during C2C12 differentiation (Chen *et al.*, 2006). These findings correspond well with the low expression level of nesprin-3 in cardiac and skeletal muscle, suggesting that a plectin-mediated link between the nucleus and IFs is not required in these tissues. Similar to that of nesprin-3, the expression level of nesprin-2 giant also decreased during myogenic differentiation. Hence attachment of the nucleus to the actin cytoskeleton is likely mediated by nesprin-1. Of interest, whereas overexpression of nesprin-3β has a dominant-negative effect on the NE localization of other KASH domain–containing proteins, it does not seem to affect myotube formation. Given that a similar observation was made by Brosig *et al.* (2010), the requirement of KASH domain–containing proteins in early myogenesis seems questionable. In contrast, KASH proteins are essential for maintenance of and mechanotransduction in muscle, as nesprin-1–mutant mice display defects in nuclear positioning and muscle function (Puckelwartz *et al.*, 2009; Zhang *et al.*, 2010).

LINC complexes were found to have a role in cell migration and polarization of MEFs (Lombardi *et al.*, 2011), but it remained undetermined which KASH domain–containing proteins were actually involved. We now demonstrate that these effects are not mediated by nesprin-3, as the absence of nesprin-3 in MEFs did not affect migration or polarization. Subsequent disruption of the remaining LINC complexes did affect polarization, suggesting the involvement of other KASH domain–containing proteins. Given that loss or knockdown of nesprin-2 giant in fibroblasts led to defects in polarization and cell migration (Lüke *et al.*, 2008; Luxton *et al.*, 2010), nesprin-2 could be the primary LINC complex component involved in these processes.

In apparent contrast to our results, Morgan *et al.* (2011) showed that flow-induced migration and polarization were reduced after small interfering RNA–mediated knockdown of nesprin-3 in human aortic endothelial cells. The discrepancy between these results might be explained by a cell type–specific effect of nesprin-3. Alternatively, the effect of nesprin-3 on migration might depend on the method used to initiate migration. Whereas flow-induced migration relies on a functional system for mechanotransduction, scratch assays might be less dependent on mechanotransduction for the initiation of migration. Of interest, Khatau *et al.* (2012) demonstrated that nesprin-2– and nesprin-3–containing LINC complexes are required for 3D, but not two-dimensional (2D), cell migration. Whereas these results partially fit our data, they do not explain the previously observed role of nesprin-2–containing LINC complexes in 2D cell migration and polarization.

In summary, we demonstrated that nesprin-3 is essential for the recruitment of plectin and vimentin to the nuclear perimeter of Sertoli cells in vivo. This link between the NE and the IF system, however, is dispensable for the function of Sertoli cells, as well as for tissue integrity in general. Future studies are required to investigate whether nesprin-3 has a role in mechanotransduction and in vivo cell migration.

MATERIALS AND METHODS

Generation of nesprin-3–knockout mice

A BAC clone comprising exons 2–4 of *Syne3* was isolated from a 129S7AB2.2 library (Sanger Institute, Hinxton, United Kingdom). A 9.2-kb fragment of genomic *Syne3* was cloned in three steps into pFlexible, which is a generic targeting vector containing the selectable marker *puroΔtk* and loxP and frt recombination sites (van der Weyden *et al.*, 2005), using sequence-specific primers containing restriction site tags (Table 1). Fragment *Syne3* I was amplified with *Pwo* polymerase using primers P3 and P4. Primers for the amplification of *Syne3* fragments II and III were P5 and P6, and P7 and P8, respectively. After linearization with *Pvu*I, 80 µg of the targeting construct was electroporated into 129/Ola-derived embryonic stem cells. Colonies resistant to 3.3 µM puromycin were screened for the desired homologous recombination by Southern blotting using a probe designed with primers P9 and P10 (Table 1). The *puroΔtk* cassette flanked by *frt* sites was removed by transient transfection of pFLPe (Rodriguez *et al.*, 2000). Colonies resistant to 5 µM ganciclovir were selected, and one recombinant embryonic stem cell clone harboring the *Syne3*-floxed allele was injected into mouse C57BL/6 blastocysts, which were transferred to mothers of the same strain. The chimeric male offspring were mated with FVB/N females. Agouti coat–colored offspring was screened for the presence of the *Syne3*-floxed allele. Mice carrying the *Syne3*-floxed allele were subsequently crossed with actin-Cre mice to generate nesprin-3–knockout mice. Offspring were screened for the absence of exon 2 by PCR analysis of tail DNA with primers P1 and P2. Heterozygous mice were intercrossed, and littermates were analyzed. The absence of nesprin-3 was verified by Western blot of tissue lysates obtained from nesprin-3 wild-type and knockout littermates.

Constructs

GFP–nesprin-3α and GFP–nesprin-3β in pLZRS-IRES-zeo were described previously (Wilhelmsen *et al.*, 2005). pLZRS-GFP was

Primer	Sequence (5′ → 3′)	Restriction sites
P1	GAGAGGCTATATGCCAAGGGGGAT	—
P2	GAGATTCCTAACAACTAGAATTAC	—
P3	TT*GGCGCGCC*GAGTGACTTACAG-GCTGTGGTC	*Asc*I
P4	TT*GGCGCGCCGATATC*GTGTCCA-GAGCTAGAAATGGGCA	*Asc*I, *Eco*RV
P5	CC*TTAATTAAATTTAAAT*TTAAGAT-TGACAGCCGTGCCGAG	*Pac*I, *Swa*I
P6	CC*TTAATTAAAGTACT*GTGGGTCCT-GAACAGAGCCAAG	*Pac*I, *Sca*I
P7	CG*CCTGCAGGAGATCTT*CCTT-GAACTTCTGGATTGGTCCA	*Sbf*I, *Bgl*II
P8	CG*CCTGCAGG*GGCTGGCCTC-GATCTCAGAAATC	*Sbf*I
P9	CATTCCTGTGGGGTATCAATGC	—
P10	AAGAACCCTTGTGTCCTACTC	—

Sequence-specific primers for *Syne3* that are used for PCR analysis of mouse tail DNA (P1 and P2), generation of a *Syne3*-specific Southern blot probe (P9 and P10), and cloning of *Syne3* (P3–P8) fragments into pFlexible. The position of restriction site tags (italic) is indicated.

TABLE 1: Primers used for the generation of nesprin-3–knockout mice.

generated by inserting the coding sequence for EGFP, derived from pEGFP-N1, into the *Bam*HI-*Not*I sites of pLZRS-IRES-zeo. Dominant-negative nesprin-1 (dnNesprin-1) in pEGFP-C2 was kindly provided by Iakowos Karakesisoglou (University of Durham, Durham City, United Kingdom; Libotte *et al.*, 2005). GFP-dnNesprin-1 was subcloned into pLZRS-IRES-zeo by inserting the dnNesprin-1 part, cut with *Eco*RI-*Sal*I, into the *Eco*RI-*Xho*I sites of LZRS. A PCR fragment encoding EGFP (generated using primers 5′-GGAATTCATGGTGAGCAAGGGCGAGG-3′ [forward] and 5′-CTCTACAAATGTGGTATGGC-3′ [reverse]) was subsequently inserted into the *Eco*RI site of LZRS-dnNesprin-1.

Isolation of MEFs

Female mice were killed at day 13.5 postcoitum. Embryos were decapitated, and soft tissues were removed. Carcasses were minced and transferred to cold phosphate-buffered saline (PBS) containing 100 U/ml penicillin and 100 U/ml streptomycin. After centrifugation, the pellet was resuspended in trypsin/EDTA and incubated overnight at 4°C. Trypsin was inactivated by addition of complete culture medium (DMEM supplemented with 10% fetal calf serum, 0.1 mM β-mercaptoethanol, 200 U/ml penicillin, and 200 U/ml streptomycin). Tissue debris was allowed to settle down for 2 min, and the MEF-containing supernatant was transferred to a tissue culture flask. MEFs were immortalized by expression of SV40 large T antigen.

Cell culture and transfection

The C2C12 murine myoblast cell line (CRL 1772; American Type Culture Collection, Manassas, VA) was maintained in DMEM (Gibco Life Technologies, Carlsbad, CA) supplemented with 20% fetal calf serum, 100 U/ml penicillin and 100 U/ml streptomycin. To induce differentiation, C2C12 myoblasts were grown to 80% confluence and placed on differentiation medium containing 2% horse serum (Yaffe and Saxel, 1977). During differentiation, cells were grown on 0.2% gelatin–coated coverslips or tissue culture plates. Ecotropic Phoenix cells were grown in DMEM supplemented with 10% fetal calf serum, 100 U/ml penicillin, and 100 U/ml streptomycin. Stable integration of GFP, GFP–nesprin-3α, GFP–nesprin-3β, and GFP–dnNesprin-1 in cells was performed as described previously (Sterk *et al.*, 2000). Briefly, retrovirus carrying the GFP constructs was produced by calcium phosphate–mediated transfection of ecotropic Phoenix packaging cells. C2C12 cells and immortalized MEFs were subsequently infected with the recombinant virus by the DOTAP (Roche, Indianapolis, IN) method, selected on Zeocin (Invitrogen, Carlsbad, CA), and sorted for the expression of GFP by fluorescence-activated cell sorting.

Cell and tissue lysates

Tissues were dissected out, submerged in liquid nitrogen, and crushed with a mortar and pestle. Crushed tissues were transferred into hot 0.1% SDS and homogenized using a Polytron mincer. The tissue lysates were boiled for 5 min and cleared by centrifugation at 20,000 × *g* for 5 min. Cells were lysed in radioimmunoprecipitation buffer consisting of 10 mM sodium phosphate, pH 7, 150 mM NaCl, 1% Nonidet P40, 1% deoxycholate, 0.1% SDS, 2 mM EDTA, 50 mM NaF, 100 μM sodium vanadate, and protease inhibitor cocktail (Sigma-Aldrich, St. Louis, MO). Lysates were cleared by centrifugation at 20,000 × *g* in a microcentrifuge at 4°C for 60 min.

Immunofluorescence

Tissues were collected from mice, embedded in Tissue-Tek O.C.T. cryoprotectant (Sakura Finetek Europe, Alphen aan den Rijn, Netherlands), and frozen in liquid nitrogen. Frozen sections were prepared, washed in PBS, and fixed in acetone (prechilled to –20°C) for 5 min. Air-dried slides were blocked with 2% bovine serum albumin (BSA) in PBS for 1 h at room temperature (RT). Cells grown on glass coverslips were fixed in 3% paraformaldehyde in PBS for 15 min, permeabilized with 0.5% Triton X-100 in PBS for 5 min, and blocked with 2% BSA in PBS. Frozen sections and cells were subsequently incubated with the primary antibody for 1 h at RT. Sections and cells were washed three times with PBS and incubated with the secondary antibody for 1 h at RT. After three washes with PBS, nuclei were stained with 4′,6-diamidino-2-phenylindole (DAPI). Frozen sections were mounted in Vectashield (Vector Laboratories, Burlingame, CA), and cells were mounted in Mowiol-DABCO. Samples were viewed under a TCS SP2 or SP5 AOBS confocal microscope (Leica, Vienna, Austria), and data were analyzed using Photoshop (Adobe, San Jose, CA) and ImageJ software (National Institutes of Health, Bethesda, MD).

Antibodies

The rabbit polyclonal antibody (pAb) against nesprin-3 and the rat monoclonal antibody (mAb) against integrin α6 (GoH3) have been described previously (Sonnenberg *et al.*, 1987; Wilhelmsen *et al.*, 2005). Mouse mAb against sarcomeric MHC (MF20) was from the Developmental Studies Hybridoma Bank (University of Iowa, Iowa City, IA). SUN2 and nesprin-2 rabbit pAbs were generously provided by Didier Hodzic (Washington University School of Medicine, St. Louis, MO). Rat mAb against laminin α1 was a kind gift of Takako Sasaki (University of Erlangen-Nürnberg, Erlangen, Germany). Other rat mAbs used in this study were MB1.2 against β1 and BMA5 against α5 (both provided by Bosco Chan, University of Western Ontario, London, Canada). Rabbit anti-vimentin and guinea pig anti-plectin (P1) were provided by Frans Ramaekers (Maastricht University Medical Center, Maastricht, Netherlands) and Harald Herrmann (German Cancer Research Center, Heidelberg, Germany). Other primary antibodies used in this study were anti-actin mouse mAb (clone C4; Chemicon International, Temecula, CA), anti-GFP mouse mAb (clone B34; Covance, Berkeley, CA), anti–lamin B goat pAb (M-20; sc-6217; Santa Cruz Biotechnology, Santa Cruz, CA), anti–γ-tubulin mouse mAb (clone GTU-88; Sigma-Aldrich), anti-vimentin rabbit mAb (D21H3; Cell Signaling, Beverly, MA), and anti-WT1 rabbit pAb (C-19; sc-192; Santa Cruz Biotechnology). The following secondary antibodies were used: donkey anti-rabbit horseradish peroxidase (HRP) (GE Healthcare, Piscataway, NJ), goat anti-mouse HRP (GE Healthcare), goat anti-rat fluorescein isothiocyanate (FITC; Rockland Immunochemicals, Gilbertsville, PA), donkey anti-mouse Texas red (Jackson ImmunoResearch, West Grove, PA), and donkey anti-rat DyLight 649 (Jackson ImmunoResearch). Goat anti-rat Texas red, goat anti–guinea pig Alexa Fluor 488, donkey anti-goat Alexa Fluor 488, goat anti-mouse Texas red, goat anti-rabbit FITC, and goat anti-rabbit Texas Red were all from Invitrogen. DAPI was purchased from Sigma-Aldrich.

Immunohistochemistry

Testes were removed, fixed for 1 d in EAF (consisting of 40% ethanol, 5% acetic acid, and 3.7% formaldehyde in PBS), and processed for sectioning. Sections were subsequently rehydrated, washed in PBS/0.05% Tween 20 (PBS-T), and subjected to antigen retrieval by heating to 95°C in 0.84 M Tris/1 mM EDTA, pH 9.0 for 30 min. After cooling down for 30 min at RT, sections were washed in PBS-T and treated for 20 min with 3% hydrogen peroxide in methanol to quench endogenous peroxidase activity. Sections were washed in PBS-T and incubated for 30 min at RT with a blocking solution

containing 1% milk powder. Thereafter sections were incubated overnight at 4°C with anti-WT1 rabbit pAb diluted 1:300 in PBS/1% BSA/1.25% normal goat serum (NGS). After three washes in PBS-T, the sections were incubated for 30 min at RT with a biotinylated goat anti-rabbit pAb (E0432; Dako, Carpinteria, CA) diluted 1:1000 in PBS/0.05% BSA. Sections were again washed in PBS-T and subsequently incubated with streptavidin/HRP (P0397; Dako) diluted 1:200 in PBS/1% BSA/1.25% NGS for a further 30 min at RT. After three 5-min washes with PBS-T, the antigen was finally detected by treating the sections with 3,3′-diaminobenzidine tetrahydrochloride, after which positive immunoreactivity was revealed as brown staining. Sections were counterstained with hematoxylin, dehydrated in 100% ethanol, and cleared in xylene. For negative controls the primary antibody was substituted by the appropriate normal serum. Sections were scanned with the ScanScope XT (Aperio, Vista, CA).

Electron microscopy

Tissues were fixed in Karnovsky's fixative, followed by postfixation with 1% osmium tetroxide in 0.1 M cacodylate buffer. After washing, the tissues were stained en bloc with Ultrastain 1 (Leica), followed by ethanol dehydration series. Finally, the tissues were embedded in a mixture of DDSA/NMA/Embed-812 (Electron Microscopy Sciences, Hatfield, PA), sectioned, stained with Ultrastain 2 (Leica), and analyzed with a CM10 electron microscope (FEI, Eindhoven, Netherlands).

Scratch assays

Cells were grown to confluence, and the monolayer was subsequently wounded by scraping with a P200 pipette tip. Phase contrast images were acquired at 20-min intervals using a Zeiss Axiovert 200M inverted microscope equipped with an AxioCam MRm Rev.2 camera (Carl Zeiss, Jena, Germany). Images were analyzed using ImageJ software. Wound closure is defined as the surface area closed per minute. To investigate cell polarization, cells were fixed in methanol either directly after application of the scratch or 3 h postwounding and stained for γ-tubulin. Polarization relative to the scratch wound was determined as described previously (Lee *et al.*, 2007). A total of 200 primary and 500 immortalized cells were analyzed per individual cell line in at least three independent scratch wounds. Comparisons were carried out with the one-way analysis of variance (ANOVA), followed by pairwise analyses using Tukey's post hoc test.

Quantification and statistics

To quantify the differentiation of C2C12 cells, we determined the differentiation index as the percentage of nuclei in MHC-positive cells over the total number of nuclei. Quantifications were performed on maximal projections of *z*-stacks. A minimum of 500 nuclei per experimental time point were counted. The distance between the MTOC and the NE was determined after staining of primary MEFs for γ-tubulin and lamin B to identify the MTOC and NE, respectively. MTOC–NE distance was determined in 200 cells per individual MEF cell line. For MTOC–NE distance and Sertoli cell nuclear positioning, comparisons between wild-type and knockout were made using the Mann–Whitney *U* test and Student's *t* test, respectively. Cells were scored as having NE-associated vimentin if filaments were found to (partially) align with the nucleus or NE. Vimentin localization was determined for 100 cells per cell line, and differences between cell lines were determined with the one-way ANOVA, followed by pairwise analyses using Tukey's post hoc test.

ACKNOWLEDGMENTS

We thank Bosco Chan, Harald Herrmann, Didier Hodzic, Iakowos Karakesisoglou, Frans Ramaekers, and Takako Sasaki for providing reagents and Dirk-Jan de Groot for assistance with the analysis of the scratch assays. This work was supported by a grant from the Netherlands Organization for Scientific Research (NWO/ALW).

REFERENCES

Amlani S, Vogl AW (1988). Changes in the distribution of microtubules and intermediate filaments in mammalian Sertoli cells during spermatogenesis. Anat Rec 220, 143–160.

Andrés V, Walsh K (1996). Myogenin expression, cell cycle withdrawal, and phenotypic differentiation are temporally separable events that precede cell fusion upon myogenesis. J Cell Biol 132, 657–666.

Aumüller G, Steinbrück M, Krause W, Wagner HJ (1988). Distribution of vimentin-type intermediate filaments in Sertoli cells of the human testis, normal and pathologic. Anat Embryol (Berl) 178, 129–136.

Brosig M, Ferralli J, Gelman L, Chiquet M, Chiquet-Ehrismann R (2010). Interfering with the connection between the nucleus and the cytoskeleton affects nuclear rotation, mechanotransduction and myogenesis. Int J Biochem Cell Biol 42, 1717–1728.

Chancellor TJ, Lee J, Thodeti CK, Lele T (2010). Actomyosin tension exerted on the nucleus through nesprin-1 connections influences endothelial cell adhesion, migration, and cyclic strain-induced reorientation. Biophys J 99, 115–123.

Chen IH, Huber M, Guan T, Bubeck A, Gerace L (2006). Nuclear envelope transmembrane proteins (NETs) that are up-regulated during myogenesis. BMC Cell Biol 7, 38.

Colucci-Guyon E, Portier MM, Dunia I, Paulin D, Pournin S, Babinet C (1994). Mice lacking vimentin develop and reproduce without an obvious phenotype. Cell 79, 679–694.

Crisp M, Liu Q, Roux K, Rattner JB, Shanahan C, Burke B, Stahl PD, Hodzic D (2006). Coupling of the nucleus and cytoplasm: role of the LINC complex. J Cell Biol 172, 41–53.

Del Rio-Tsonis K, Covarrubias L, Kent J, Hastie ND, Tsonis PA (1996). Regulation of the Wilms' tumor gene during spermatogenesis. Dev Dyn 207, 372–381.

Ding X, Xu R, Yu J, Xu T, Zhuang Y, Han M (2007). SUN1 is required for telomere attachment to nuclear envelope and gametogenesis in mice. Dev Cell 12, 863–872.

Durbeej M, Henry MD, Ferletta M, Campbell KP, Ekblom P (1998). Distribution of dystroglycan in normal adult mouse tissues. J Histochem Cytochem 46, 449–457.

Fan J, Beck KA (2004). A role for the spectrin superfamily member Syne-1 and kinesin II in cytokinesis. J Cell Sci 117, 619–629.

Franke WW, Grund C, Schmid E (1979). Intermediate-sized filaments present in Sertoli cells are of the vimentin type. Eur J Cell Biol 19, 269–275.

Fuchs E, Cleveland DW (1998). A structural scaffolding of intermediate filaments in health and disease. Science 279, 514–519.

Geerts D, Fontao L, Nievers MG, Schaapveld RQ, Purkis PE, Wheeler GN, Lane EB, Leigh IM, Sonnenberg A (1999). Binding of integrin a6b4 to plectin prevents plectin association with F-actin but does not interfere with intermediate filament binding. J Cell Biol 147, 417–434.

Göb E, Schmitt J, Benavente R, Alsheimer M (2010). Mammalian sperm head formation involves different polarization of two novel LINC complexes. PLoS One 5, e12072.

Grady RM, Starr DA, Ackerman GL, Sanes JR, Han M (2005). Syne proteins anchor muscle nuclei at the neuromuscular junction. Proc Natl Acad Sci USA 102, 4359–4364.

Guttman JA, Mulholland DJ, Vogl AW (1999). Plectin is concentrated at intercellular junctions and at the nuclear surface in morphologically differentiated rat Sertoli cells. Anat Rec 254, 418–428.

Häger M, Gawlik K, Nyström A, Sasaki T, Durbeej M (2005). Laminin a1 chain corrects male infertility caused by absence of laminin a2 chain. Am J Pathol 167, 823–833.

Haque F, Lloyd DJ, Smallwood DT, Dent CL, Shanahan CM, Fry AM, Trembath RC, Shackleton S (2006). SUN1 interacts with nuclear lamin A and cytoplasmic nesprins to provide a physical connection between the nuclear lamina and the cytoskeleton. Mol Cell Biol 26, 3738–3751.

Hess RA, Renato de Franca L (2008). Spermatogenesis and cycle of the seminiferous epithelium. Adv Exp Med Biol 636, 1–15.

Horn HF *et al.* (2013). The LINC complex is essential for hearing. J Clin Invest 123, 740–750.

Kandert S *et al*. (2007). Nesprin-2 giant safeguards nuclear envelope architecture in LMNA S143F progeria cells. Hum Mol Genet 16, 2944–2959.
Ketema M, Sonnenberg A (2011). Nesprin-3: a versatile connector between the nucleus and the cytoskeleton. Biochem Soc Trans 39, 1719–1724.
Ketema M, Wilhelmsen K, Kuikman I, Janssen H, Hodzic D, Sonnenberg A (2007). Requirements for the localization of nesprin-3 at the nuclear envelope and its interaction with plectin. J Cell Sci 120, 3384–3394.
Khatau SB *et al*. (2012). The distinct roles of the nucleus and nucleus-cytoskeleton connections in three-dimensional cell migration. Sci Rep 2, 488.
Lee JS, Hale CM, Panorchan P, Khatau SB, George JP, Tseng Y, Stewart CL, Hodzic D, Wirtz D (2007). Nuclear lamin A/C deficiency induces defects in cell mechanics, polarization, and migration. Biophys J 93, 2542–2552.
Libotte T *et al*. (2005). Lamin A/C-dependent localization of nesprin-2, a giant scaffolder at the nuclear envelope. Mol Biol Cell 16, 3411–3424.
Lombardi ML, Jaalouk DE, Shanahan CM, Burke B, Roux KJ, Lammerding J (2011). The interaction between nesprins and sun proteins at the nuclear envelope is critical for force transmission between the nucleus and cytoskeleton. J Biol Chem 286, 26743–26753.
Lüke Y *et al*. (2008). Nesprin-2 Giant (NUANCE) maintains nuclear envelope architecture and composition in skin. J Cell Sci 121, 1887–1898.
Luxton GW, Gomes ER, Folker ES, Vintinner E, Gundersen GG (2010). Linear arrays of nuclear envelope proteins harness retrograde actin flow for nuclear movement. Science 329, 956–959.
Magin TM, Hesse M, Schröder R (2000). Novel insights into intermediate-filament function from studies of transgenic and knockout mice. Protoplasma 211, 140–150.
McLean WH *et al*. (1996). Loss of plectin causes epidermolysis bullosa with muscular dystrophy: cDNA cloning and genomic organization. Genes Dev 10, 1724–1735.
Morgan JT, Pfeiffer ER, Thirkill TL, Kumar P, Peng G, Fridolfsson HN, Douglas GC, Starr DA, Barakat AI (2011). Nesprin-3 regulates endothelial cell morphology, perinuclear cytoskeletal architecture, and flow-induced polarization. Mol Biol Cell 22, 4324–4334.
Morimoto A, Shibuya H, Zhu X, Kim J, Ishiguro K, Han M, Watanabe Y (2012). A conserved KASH domain protein associates with telomeres, SUN1, and dynactin during mammalian meiosis. J Cell Biol 198, 165–172.
Myers M, Ebling FJ, Nwagwu M, Boulton R, Wadhwa K, Stewart J, Kerr JB (2005). Atypical development of Sertoli cells and impairment of spermatogenesis in the hypogonadal (hpg) mouse. J Anat 207, 797–811.
Padmakumar VC, Abraham S, Braune S, Noegel AA, Tunggal B, Karakesisoglou I, Korenbaum E (2004). Enaptin, a giant actin-binding protein, is an element of the nuclear membrane and the actin cytoskeleton. Exp Cell Res 295, 330–339.
Padmakumar VC, Libotte T, Lu W, Zaim H, Abraham S, Noegel AA, Gotzmann J, Foisner R, Karakesisoglou I (2005). The inner nuclear membrane protein Sun1 mediates the anchorage of nesprin-2 to the nuclear envelope. J Cell Sci 118, 3419–3430.
Postel R, Ketema M, Kuikman I, de Pereda JM, Sonnenberg A (2011). Nesprin-3 augments peripheral nuclear localization of intermediate filaments in zebrafish. J Cell Sci 124, 755–764.
Puckelwartz MJ *et al*. (2009). Disruption of nesprin-1 produces an Emery Dreifuss muscular dystrophy-like phenotype in mice. Hum Mol Genet 18, 607–620.
Rashmi RN *et al*. (2012). The nuclear envelope protein nesprin-2 has roles in cell proliferation and differentiation during wound healing. Nucleus 3, 172–186.
Razafsky D, Hodzic D (2009). Bringing KASH under the SUN: the many faces of nucleo-cytoskeletal connections. J Cell Biol 186, 461–472.
Rodriguez CI, Buchholz F, Galloway J, Sequerra R, Kasper J, Ayala R, Stewart AF, Dymecki SM (2000). High-efficiency deleter mice show that FLPe is an alternative to Cre-loxP. Nat Genet 25, 139–140.
Rosenthal N (1989). Muscle cell differentiation. Curr Opin Cell Biol 1, 1094–1101.
Roux KJ, Crisp ML, Liu Q, Kim D, Kozlov S, Stewart CL, Burke B (2009). Nesprin 4 is an outer nuclear membrane protein that can induce kinesin-mediated cell polarization. Proc Natl Acad Sci USA 106, 2194–2199.
Schmitt J, Benavente R, Hodzic D, Höög C, Stewart CL, Alsheimer M (2007). Transmembrane protein Sun2 is involved in tethering mammalian meiotic telomeres to the nuclear envelope. Proc Natl Acad Sci USA 104, 7426–7431.
Schneider M, Lu W, Neumann S, Brachner A, Gotzmann J, Noegel AA, Karakesisoglou I (2011). Molecular mechanisms of centrosome and cytoskeleton anchorage at the nuclear envelope. Cell Mol Life Sci 68, 1593–1610.
Siu MK, Cheng CY (2004). Dynamic cross-talk between cells and the extracellular matrix in the testis. Bioessays 26, 978–992.
Sonnenberg A, Janssen H, Hogervorst F, Calafat J, Hilgers J (1987). A complex of platelet glycoproteins Ic and IIa identified by a rat monoclonal antibody. J Biol Chem 262, 10376–10383.
Sonnenberg A, Liem RK (2007). Plakins in development and disease. Exp Cell Res 313, 2189–2203.
Starr DA, Fridolfsson HN (2010). Interactions between nuclei and the cytoskeleton are mediated by SUN-KASH nuclear-envelope bridges. Annu Rev Cell Dev Biol 26, 421–444.
Sterk LM, Geuijen CA, Oomen LC, Calafat J, Janssen H, Sonnenberg A (2000). The tetraspan molecule CD151, a novel constituent of hemidesmosomes, associates with the integrin a6b4 and may regulate the spatial organization of hemidesmosomes. J Cell Biol 149, 969–982.
Stewart-Hutchinson PJ, Hale CM, Wirtz D, Hodzic D (2008). Structural requirements for the assembly of LINC complexes and their function in cellular mechanical stiffness. Exp Cell Res 314, 1892–1905.
van der Weyden L, Adams DJ, Harris LW, Tannahill D, Arends MJ, Bradley A (2005). Null and conditional semaphorin 3B alleles using a flexible puroDeltatk loxP/FRT vector. Genesis 41, 171–178.
Vogl AW, Colucci-Guyon E, Babinet C (1996). Vimentin intermediate filaments are not necessary for the development of a normal differentiated phenotype by mature Sertoli cells. Mol Biol Cell 7, 555a.
Wang N, Tytell JD, Ingber DE (2009). Mechanotransduction at a distance: mechanically coupling the extracellular matrix with the nucleus. Nat Rev Mol Cell Biol 10, 75–82.
Wiche G (1998). Role of plectin in cytoskeleton organization and dynamics. J Cell Sci 111, 2477–2486.
Wilhelmsen K, Litjens SH, Kuikman I, Tshimbalanga N, Janssen H, van den Bout I, Raymond K, Sonnenberg A (2005). Nesprin-3, a novel outer nuclear membrane protein, associates with the cytoskeletal linker protein plectin. J Cell Biol 171, 799–810.
Wrobel KH, Mademann R, Sinowatz F (1979). The lamina propria of the bovine seminiferous tubule. Cell Tissue Res 202, 357–377.
Yaffe D, Saxel O (1977). Serial passaging and differentiation of myogenic cells isolated from dystrophic mouse muscle. Nature 270, 725–727.
Yu J, Lei K, Zhou M, Craft CM, Xu G, Xu T, Zhuang Y, Xu R, Han M (2011). KASH protein Syne-2/nesprin-2 and SUN proteins SUN1/2 mediate nuclear migration during mammalian retinal development. Hum Mol Genet 20, 1061–1073.
Zhang J *et al*. (2010). Nesprin 1 is critical for nuclear positioning and anchorage. Hum Mol Genet 19, 329–341.
Zhang Q, Ragnauth CD, Skepper JN, Worth NF, Warren DT, Roberts RG, Weissberg PL, Ellis JA, Shanahan CM (2005). Nesprin-2 is a multi-isomeric protein that binds lamin and emerin at the nuclear envelope and forms a subcellular network in skeletal muscle. J Cell Sci 118, 673–687.
Zhang Q, Skepper JN, Yang F, Davies JD, Hegyi L, Roberts RG, Weissberg PL, Ellis JA, Shanahan CM (2001). Nesprins: a novel family of spectrin-repeat-containing proteins that localize to the nuclear membrane in multiple tissues. J Cell Sci 114, 4485–4498.
Zhang X, Lei K, Yuan X, Wu X, Zhuang Y, Xu T, Xu R, Han M (2009). SUN1/2 and Syne/Nesprin-1/2 complexes connect centrosome to the nucleus during neurogenesis and neuronal migration in mice. Neuron 64, 173–187.
Zhang X, Xu R, Zhu B, Yang X, Ding X, Duan S, Xu T, Zhuang Y, Han M (2007). Syne-1 and Syne-2 play crucial roles in myonuclear anchorage and motor neuron innervation. Development 134, 901–908.
Zhen YY, Libotte T, Munck M, Noegel AA, Korenbaum E (2002). NUANCE, a giant protein connecting the nucleus and actin cytoskeleton. J Cell Sci 115, 3207–3222.
Zhu LJ, Zong SD, Phillips DM, Moo-Young AJ, Bardin CW (1997). Changes in the distribution of intermediate filaments in rat Sertoli cells during the seminiferous epithelium cycle and postnatal development. Anat Rec 248, 391–405.